Chapter 4

Varied Weight Linear Carboxylic and Dicarboxylic Acids in Carbon Black Composite Vapor Sensors

4.1 Abstract

Varied length carboxylic (C10–C24) and dicarboxylic (C2–C14) acids have been tested in small molecule/carbon black composite chemiresistor sensors. Minor chain length effects were noted in the dicarboxylic acid series, and the smallest molecule in each series provided unpredictable responses. Carboxylic acid arrays provided greater discriminatory ability than dicarboxylic arrays. This benefit possibly accrues from the greater availability of both carboxyl and alkyl groups in the carboxylic acids, suggesting future use of different multi-functional group small molecules in thin film vapor sensors.

4.2 Introduction

Arrays of resistive thin film vapor sensors have found use in fields as diverse as environmental monitoring,[1,2] disease diagnostics,[3,4] food quality control,[5,6] and explosives detec-

tion.[7,8] Systems such as intrinsically conducting polymers,[9,10] ligand-capped metal nanoparticles,[11–13] and organic insulators mixed with a conductor such as carbon nanotubes[14,15] or carbon black[16–18] have all been explored. Varying the chemical functionality present among the detectors in the array ensures a widely responding and finely discriminating system. Each sensor in such an array provides a varying set of responses to different classes of analyte vapors, thus creating distinct patterns of response when the array response is taken as a whole.

Composite sensor films of insulating polymers mixed with carbon black have been broadly investigated in our lab,[16,19–21] and more recently, the use of a variety of non-volatile small organic compounds instead of polymers has been examined.[18] Sensors made of these composite films work by a swelling mechanism. Adsorption of an analyte vapor into the film causes the insulating phase to expand, increasing the average distance between the conductive carbon black (CB) particles, and causing a rapid, reversible change in the film resistance.[19]

As compared to the polymer composite films, increased functional group density and disordered arrangement in small molecule composite films has been proposed to allow greater vapor permeability and increased analyte-sensor interactions, making these materials engaging sensor candidates. Small molecule composite films have generally exhibited highest signal-to-noise (SNR) ratios in mixtures containing 60–75 wt% of CB, whereas polymer composites perform best at the much lower levels of 20–40 wt% of CB. Investigations have suggested (Chapter 2) that the inherent crystallinity of the small molecule films impedes their ability to swell. In turn, the larger quantities of CB relative to the polymer

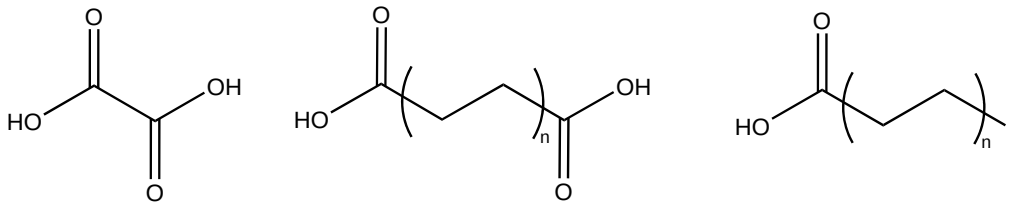

oxalic acid dicarboxylic acids carboxylic acids

Figure 4.1: Images of the basic structures of the carboxylic and dicarboxylic acids used.

films are necessary to to break up the large scale crystalline features in small molecule films. Differences in the size and polarity of the small molecules has been proposed to affect the requirements and responses of each small molecule.

In this study, two related homologous series of molecules have been used to prepare composite vapor sensors. Incorporating *n*-alkyl carboxylic and α, ω-dicarboxylic acids of varied length into vapor sensor arrays (referred to hereinafter as carboxylic and dicarboxylic acids, Figure 4.1, Table 4.1) allows investigation of the effects of controllably varied length differences — in each series, the ratio of alkyl to carboxylic groups steadily changes as the overall chain length increases. Additionally, the effects of mono- versus di-terminal strongly H-bonding groups are explored. Use of only the C_{2n} acids avoids any confounding effects from the even-odd variations seen in such molecules.[22,23]

Single sensor responses and overall array discrimination will be explored for these organic acid/CB composite sensor films. Additionally, their mass sorption and swelling behaviors will be examined through the use of quartz crystal microbalance (QCM) measurements and ellipsometry.

Acid Compound	C_n (n)	MW (g/mol)	mp (°C)	ρ (g/cm^3)
oxalic	2	90.04	190	1.90
succinic	4	118.09	186	1.56
adipic	6	146.14	153	1.36
suberic	8	174.20	140	1.27
sebacic	10	202.25	131	1.21
dodecanedioic	12	230.31	128	1.15
tetradecanedioic	24	258.36	127	1.08
decanoic	10	172.27	32	0.9
myristic	14	228.38	54	0.86
palmitic	16	256.43	62	0.85
stearic	18	284.48	69	0.85
tetracosanoic	24	368.65	80	0.85

Table 4.1: Listing and physical characteristics of all small molecules used in this study. Values are number of carbon atoms in molecule backbone, molecular weight, melting point, and density.

4.3 Experimental

4.3.1 Materials

All carboxylic and dicarboxylic acids, as well as dioctyl phthalate (DOP) were acquired from Sigma-Aldrich (Figure 4.1, Table 4.1). Except for stearic acid (95%), all compounds purchased were of 98% purity or greater. Gold wire (0.25 mm diam., 99.9+%) was also purchased from Sigma-Aldrich. Reagent grade hexane, heptane, chloroform, isopropanol, ethanol, ethyl acetate, and tetrahydrofuran were acquired from VWR. Chromium metal was purchased from RD Matthes. Black Pearls 2000, a carbon black (CB) material, was donated by Cabot Co. (Billerica, MA). All materials were used as received.

4.3.2 Sample Preparation

Sensor substrates were prepared by thermal evaporation of layered Cr (30 nm) and Au leads (60 nm) onto glass slides, after which the slide was cut into 0.5 cm x 2.5 cm pieces, as previously described (Section 2.3.2). The substrates for QCM measurements were 10 MHz polished quartz crystals (International Crystal Manufacturing). Each crystal contained a 0.201″ diameter electrode of 100 nm of Au on top of 10 nm of Cr. Ellipsometry samples were deposited onto cleaned pieces of polished silicon wafer.

All sensor solutions and mixtures were prepared in 20 mL of THF. In all cases, the organic acid and DOP, if used, were first dissolved in the solvent. The appropriate mass of carbon black was then added, and the mixture sonicated for at least 30 minutes to adequately disperse the CB particles. Mixtures with CB contained a total of 200 mg of solid materials, in three different ratios — one at 75 weight percent (wt %) CB, and two at 40 wt% CB (Table 4.2). Additionally, solutions were prepared from the pure acid, or the acid mixed in a 3:1 mass ratio with the plasticizer material.

Sensors and QCM films were prepared from each CB-containing mixture, while pure acid and acid/DOP solutions were used to prepare QCM and ellipsometry films. Two mixtures were made of each CB-containing formulation. Two sensors were deposited from each mixture, and QCM films were also prepared from both mixtures.

Sensor and QCM films were deposited via airbrush onto sensor slides or QCM crystals (Section 2.3.2). Ellipsometry samples were deposited via spin coater onto pieces of silicon wafer, yielding homogenous, optically smooth surfaces. The baseline frequency of each QCM crystal was noted prior to film deposition. All QCM samples were placed in a vacuum

Label	Acid (mg)	Plasticizer (mg)	Carbon Black (mg)
75	50	0	150
40	120	0	80
40/p	90	30	80

Table 4.2: Composition of all CB-containing mixtures used. The first column lists the abbreviation used in the manuscript to denote each type of film composition.

desiccator for at least 2 h prior to use. The frequency shift caused by deposition of the film was recorded immediately prior to data acquisition.

4.3.3 Measurements and Data Analysis

4.3.3.1 Chemiresistive Sensors

The sensors in an array were placed in an airtight PTFE and stainless steel flow chamber, and connected via Teflon tubing to a computer controlled vapor generation and delivery system (Section 2.3.3.1). The sensors were initially exposed to 2.5 L min^{-1} flow of air for a time period sufficient to stabilize their baseline resistances.

Seven analytes (hexane, heptane, chloroform, ethanol, isopropanol, ethyl acetate, and toluene) were used to test the sensors. All analytes were presented at a fraction saturation of $P/P^0 = 0.01$ (where P is the partial pressure and P^0 is the vapor pressure of the analyte at room temperature). Analytes were presented 25 times each to the sensor array, with the exposure order of the analytes randomized to minimize potential effects of sensor hysteresis. Each analyte exposure consisted of 100 seconds of laboratory air, 200 seconds of analyte, and a final 100 second purge of laboratory air. Data collection runs were performed at least four times on each sensor array. Reported data is from the final set of exposures.

The resistance of each sensor was measured approximately every 5 s. For each analyte exposure to each sensor, the data were first baseline corrected, and a single value, $\Delta R_{\text{max}}/R_{\text{b}}$ (the relative change in resistance) was extracted. R_{b} is the steady-state baseline resistance of the sensor and ΔR_{max} is the maximum resistance change observed during exposure to the analyte. A signal-to-noise ratio (SNR) was also determined for each exposure, with the SNR value defined as ΔR_{max} divided by the standard deviation of the data points used to calculate R_{b}. SNR and $\Delta R_{\text{max}}/R_{\text{b}}$ were calculated as previously reported (Section 2.3.3.1). This work uses principal components analysis (PCA) to visualize how well the sensor arrays distinguish between different analytes.[24] PCA rotates the data such that the first few dimensions contain as much as possible of the variance contained in the entirety of the array response. All data analysis was performed in MATLAB.

4.3.4 QCM Measurements

Coated QCM crystals were mounted in a sealed chamber and exposed to analytes using a setup very similar to that of the chemiresistive sensors (Section 2.3.3.2). The QCM chamber holds only one crystal, and as such, the QCM films were examined consecutively, not in arrays. Each crystal was first exposed to a baseline period of background air, followed by the analyte exposures. Each analyte exposure consisted of a 200 s period of air, followed by 100 s of analyte, followed by another 200 s of air.

Hexane, chloroform, and toluene were the analytes used for QCM experiments. Each crystal was exposed to a random ordering of 10 exposures of each analyte. All analytes were presented at an analyte partial pressure of $P/P^0 = 0.01$. At least two complete sets

of exposures were presented to each film.

The mass of the deposited sensor film causes a shift in the frequency of the QCM crystal Δf_{f}, and each exposure to an analyte causes a further frequency shift, Δf_{a}. Changes of resonant frequency of a coated crystal can be referenced to changes in mass through the Sauerbrey equation (Section 2.3.3.2), which directly relates the two. This allows determination of the analyte mass absorbed per unit mass of the deposited film, $\Delta m_{\mathrm{a}}/m_{\mathrm{f}}$. This value was calculated for each exposure to analyte for each film.

4.3.5 Ellipsometry

Ellipsometry was performed with a Gaertner L116C system. Samples for ellipsometry were placed in a plastic chamber with a drilled opening at each end to allow the laser beam to reach the sample and detector unimpeded. Baseline thickness readings were collected under a steady 65 mL min^{-1} stream of air, with an adjacent ventilation tube used to flush the chamber. Exposures to saturated hexane vapor at 65 mL min^{-1} were initiated by hand. During the exposures the ventilation tube was removed, to encourage maximum retention of hexane in the chamber. The purge and exposure times were each $\geq$5 min. Each sample was exposed a minimum of five times, and at least five data points were measured during and between each exposure. These data points were averaged to yield the relative thickness change of the film for each analyte exposure.

4.4 Results

4.4.1 Chemiresistive Sensors

4.4.1.1 Dicarboxylic Acids

All length dicarboxylic acid sensors responded at all formulations. $\Delta R/R_b$ and SNR values are summarized in Tables 4.3 and 4.4. $\Delta R/R_b$ were generally higher at 75 CB than the other two formulations, and SNR levels were lower at 40/p than in either of the other formulations. $\Delta R/R_b$ responses were highest to toluene at both 40 and 75 CB, while at 40/p responses to $CHCl_3$ notably increased. Responses of C4–C8 acids to the hydrocarbon analytes (toluene, hexane, heptane) were larger than those of the longer chains by 40% or more at all formulations, and 10–20% higher to oxygen containing analytes at 75 CB. Oxalic (C2) acid had widely variable responses, with response profiles of a given sensor changing over time. At 75 CB, responses changed from negative to positive over 6 days for several analytes (Figures 4.2). A similar but smaller effect for $CHCl_3$ and EtOAc was seen at 40 CB, and not seen at 40/p.

Single response curves (Figures 4.3–4.5) of dicarboxylic acids at all three formulations show the overall rapidity of response of all sensors. Curve shapes are similar at 75 and 40 CB, becoming slightly less rapid for chloroform at 40/p. These also display the variegated C2 responses.

PCA plots of dicarboxylic acid sensor arrays (Figures 4.9–4.11) show that the arrays successfully discriminate chloroform, clearly separate the hydrocarbons from the oxygen-containing analytes, and separate hexane from heptane (although they remain close). For-

mulations at 75 and 40 wt% of CB also clearly separate toluene from all other analytes, while at 40/p toluene is much less well separated from hexane/heptane. In no cases are the oxygen-containing analytes differentiated from each other. Both dicarboxylic 40 and 75 CB captured over 90% of the total variance in the first three principal components, whereas 40/p captured only 70% in the first three PCs.

4.4.1.2 Carboxylic Acids

All carboxylic acids responded at all formulations. $\Delta R/R_b$ and SNR values are summarized in Tables 4.5 and 4.6. $\Delta R/R_b$ values at 75 CB for C14–C24 are notably higher than at 40 CB and 40/p. All compounds show an improvement in response to $CHCl_3$ at 40/p compared to 40 CB, and C14–C18 also show an improvement to the hydrocarbon analytes. Except to chloroform, the responses of C24 remain the same or drop upon the switch from 40 CB to 40/p. In all three formulations, the responses of C10 are notably higher than all other weights at that formulation. The responses of C14 carboxylic acid are lower than that of C14 dicarboxylic acid to all oxygen-containing compounds, at all formulations, and lower to $CHCl_3$ at both 40 CB formulations. C14 carboxylic acid returns higher $\Delta R/R_b$ values to the hydrocarbon analytes at 75 CB than C14 dicarboxylic acid, and they produced comparable responses at both 40 CB formulations.

Single response curves for carboxylic acids at all formulations (Figures 4.6–4.8) show the overall speed of the sensor responses. They also highlight the greatly increased response of C10 carboxylic acid compared to the other lengths, and the overall similarity of the responses of the other carboxylic acids.

PCA plots of carboxylic acid sensor arrays (Figures 4.12–4.14) are more divergent than

those of the dicarboxylic acid arrays. The 75 CB plot is similar, clearly separating toluene and $CHCl_3$ from the hexane/heptane and oxygen containing clusters. The 40 CB plot has all analytes more closely together, but starts to show some separation between the oxygen-containing analytes. At 40/p, toluene, $CHCl_3$, hexane and heptane are all clearly separated from all other analytes. The three remaining analytes (EtOAc, EtOH, and iPrOH) all show some remaining overlap, but are loosely separated into three broad bands. All plots have from 80–90% of the total variance in the first three PCs.

4.4.2 QCM Responses

All films containing carbon black displayed rapid, clean mass uptake responses. 75 CB films generally displayed the largest $\Delta m_{\mathrm{a}}/m_{\mathrm{f}}$ of all CB-containing films. Responses of acid/plasticizer films were smaller than those of the CB-containing films, although $\Delta m_{\mathrm{a}}/m_{\mathrm{f}}$ values in response to $CHCl_3$ approached those of 40 CB and 40/p films. Responses of pure acid films were extremely small, with many displaying absolute frequency shifts of $\leq$2 Hz — in comparison, bare crystals show shifts of 0.5–1.5 Hz upon exposure to the same analytes. All film responses were rapid, and complete within the 100 s exposure period.

4.4.3 Ellipsometry

All films displayed responses to saturated hexane vapor. Pure films, however, displayed apparent thickness changes of 4–6 Å, similar to the nominal thickness change indicated by the change in signal displayed by a blank silicon sample wafer upon exposure to analyte. Film deposition volumes were generally equal, but not rigorously controlled. However,

mixed acid/plasticizer films were generally thicker than the pure acid films. (Table 4.7).

Mixed acid/plasticizer films swelled in the range of 4–8%, for overall shifts of 20–35 Å. Pure plasticizer films swelled $\sim$20% of their original thickness, a change of 30–40 Å. Film baselines were stable, shifting $\leq$2% of their total value over all exposures, in most cases.

Oxalic acid films were thinner than all other films, and oxalic acid/plasticizer films displayed larger percent changes than did the other mixed films, although absolute changes were similar. Pure decanoic acid and decanoic acid/plasticizer films cast via spin coater were too unstable to perform ellipsometry measurements.

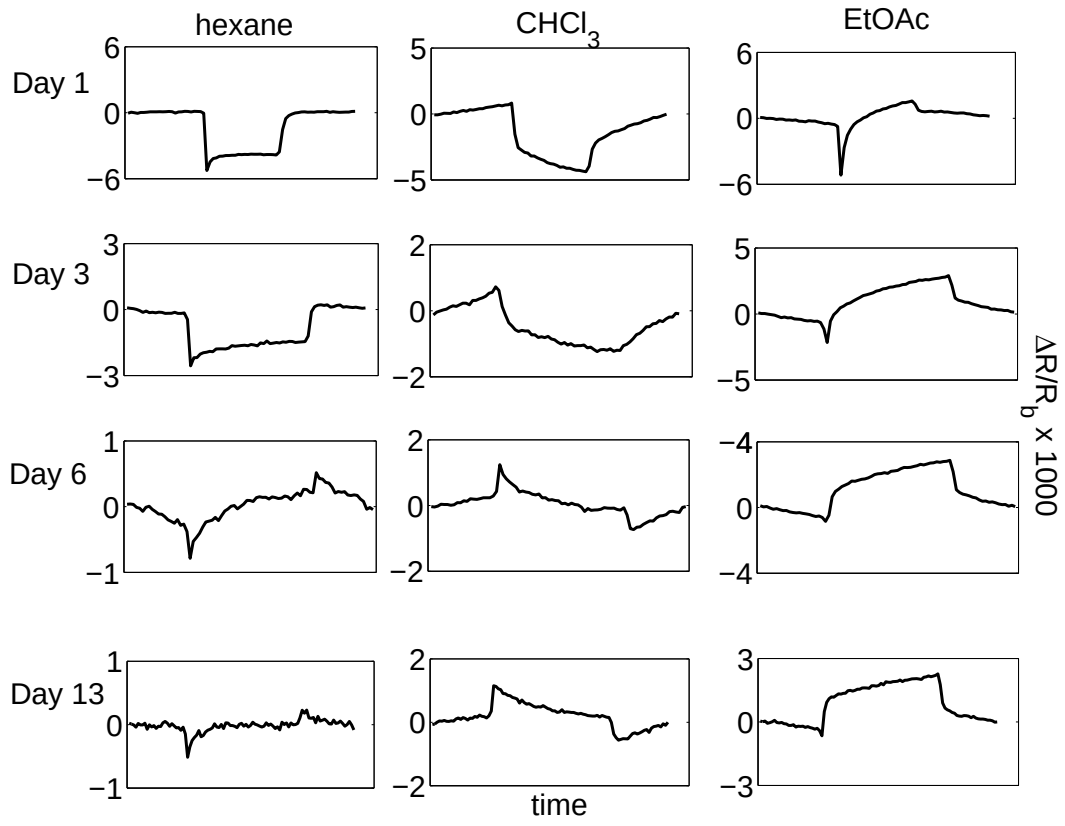

Figure 4.2: Single sensor responses of oxalic acid 75 CB to hexane, chloroform, and ethyl acetate on day 1, 3, 6 and 13 after creation. Day 1 exposure is for 100 s, all others are for 200 s. All exposures are at $P/P^0 = 0.01$, in a total 2.5 L min^{-1} flow of air.

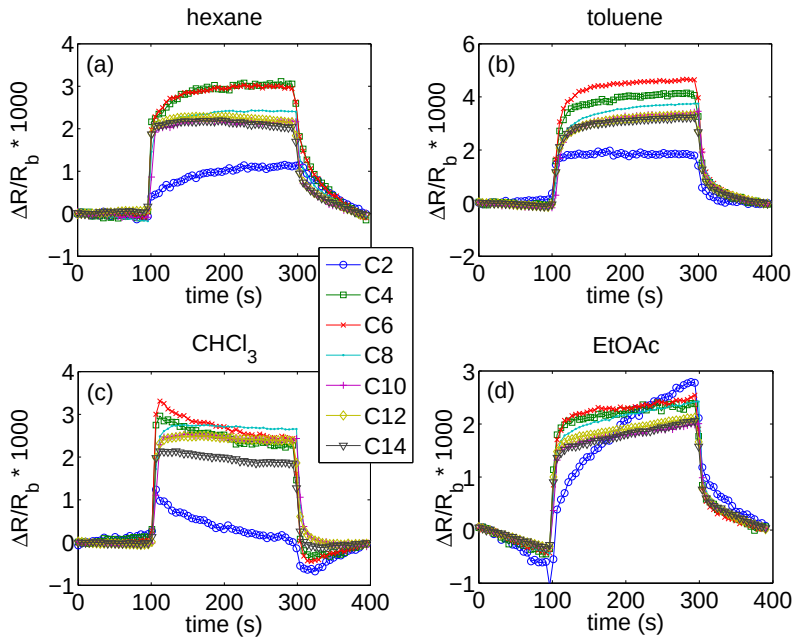

Figure 4.3: $\Delta R/R_b$ values of 200 second single exposures of dicarboxylic acid 75 CB to a) hexane, b) toluene, c) $CHCl_3$, and d) ethyl acetate. Each analyte was presented at $P/P^0 = 0.01$, in a total 2.5 L min^{-1} flow of air.

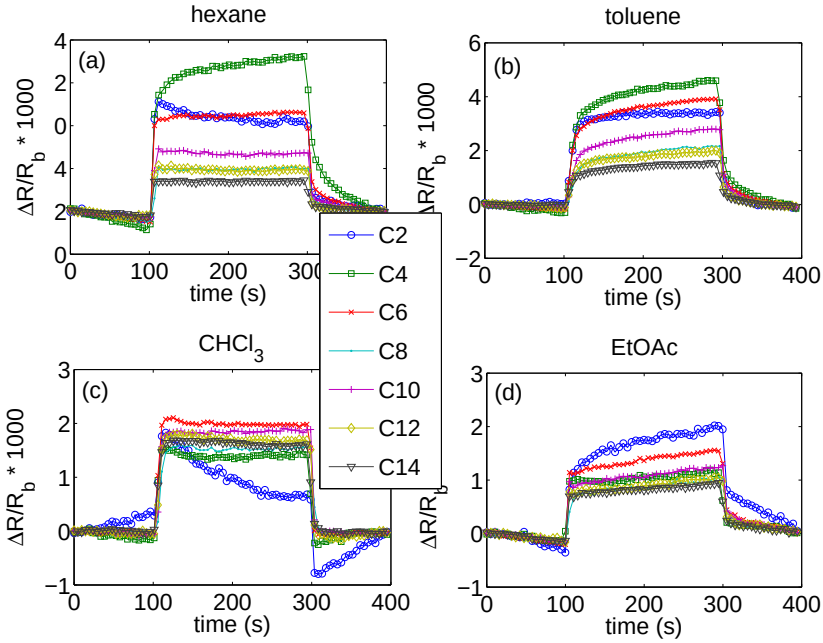

Figure 4.4: $\Delta R/R_b$ values of 200 second single exposures of dicarboxylic acid 40 CB to a) hexane, b) toluene, c) $CHCl_3$,and d) ethyl acetate. Each analyte was presented at $P/P^0 = 0.01$, in a total 2.5 L min^{-1} flow of air.

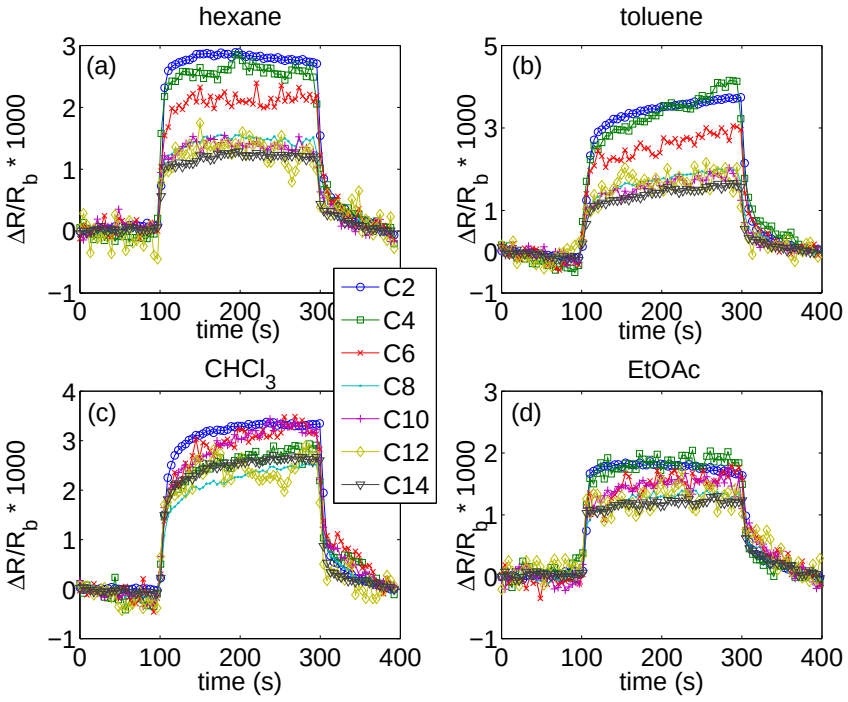

Figure 4.5: $\Delta R/R_b$ values of 200 second single exposures of dicarboxylic acid 40/p to a) hexane, b) toluene, c) $CHCl_3$, and d) ethyl acetate. Each analyte was presented at $P/P^0 = 0.01$, in a total 2.5 L min^{-1} flow of air.

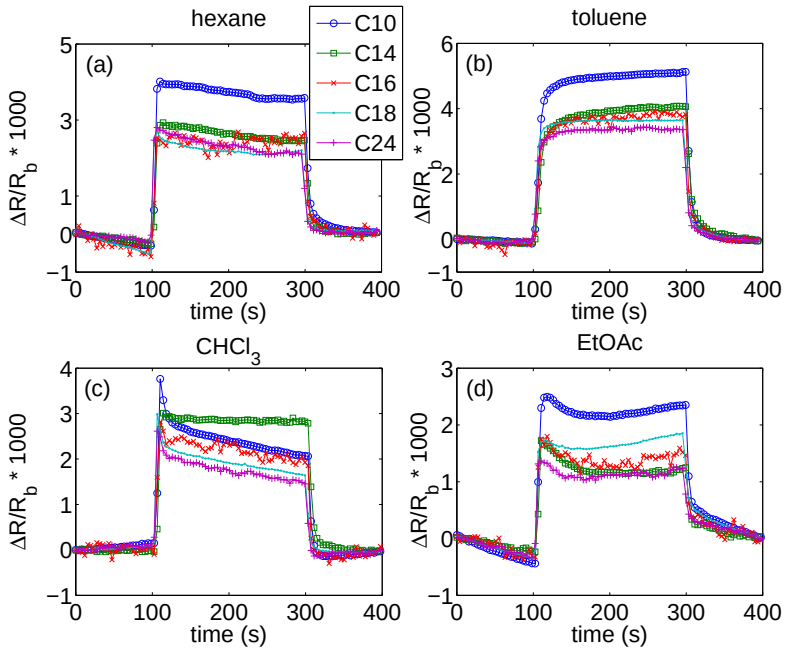

Figure 4.6: $\Delta R/R_b$ values of 200 second single exposures of carboxylic acid 75 CB to a) hexane, b) toluene, c) $CHCl_3$, and d) ethyl acetate. Each analyte was presented at $P/P^0 = 0.01$, in a total 2.5 L min^{-1} flow of air.

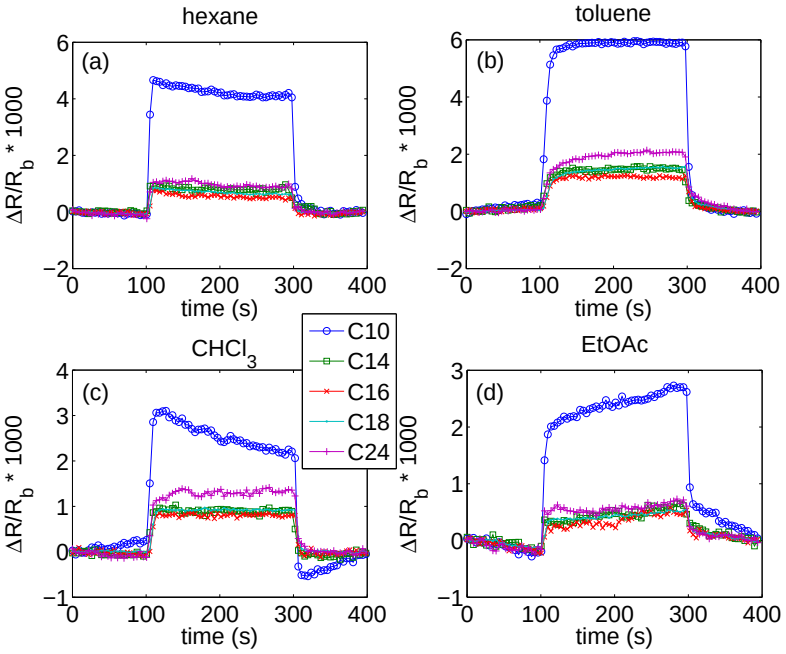

Figure 4.7: $\Delta R/R_b$ values of 200 second single exposures of carboxylic acid 40 CB to a) hexane, b) toluene, c) $CHCl_3$, and d) ethyl acetate. Each analyte was presented at $P/P^0 = 0.01$, in a total 2.5 L min^{-1} flow of air.

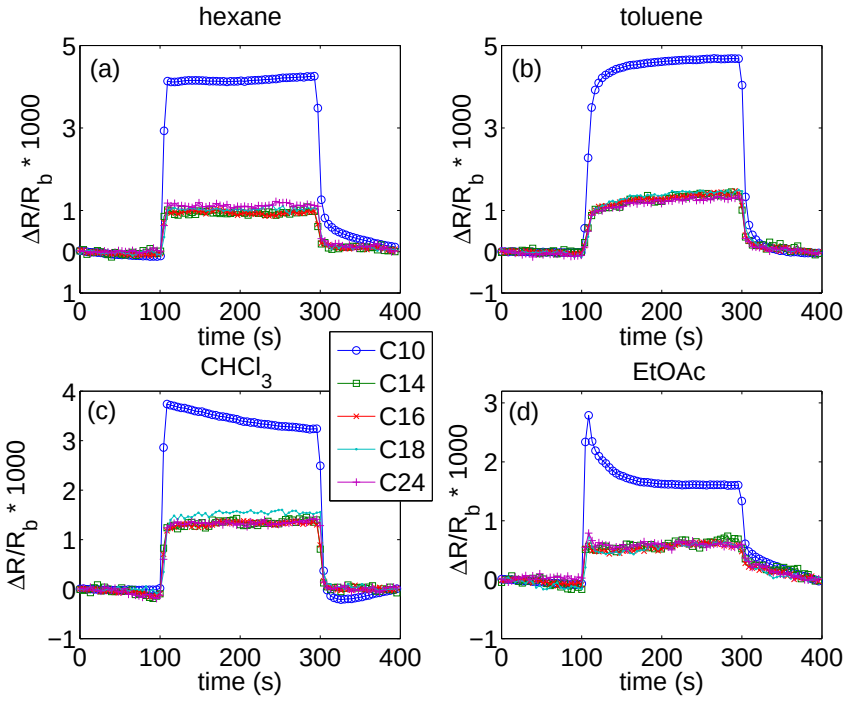

Figure 4.8: $\Delta R/R_b$ values of 200 second single exposures of carboxylic acid 40/p to a) hexane, b) toluene, c) $CHCl_3$, and d) ethyl acetate. Each analyte was presented at $P/P^0 = 0.01$, in a total 2.5 L min^{-1} flow of air.

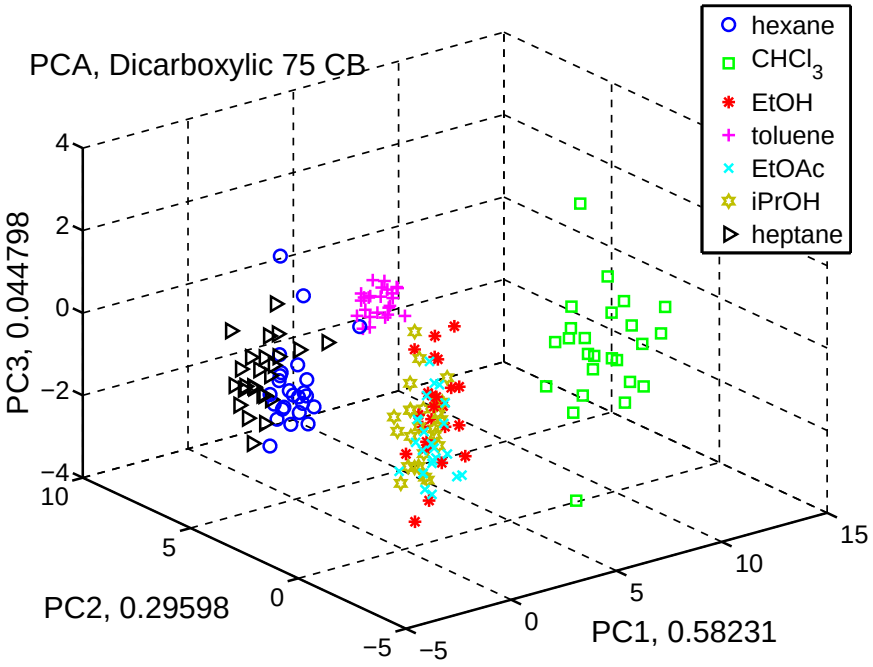

Figure 4.9: PCA plot of dicarboxylic acid 75 CB sensors. There are 25 exposures to each analyte. Numbers next to each principal component axis reflect the percentage of the total sensor response variance contained in that principal component

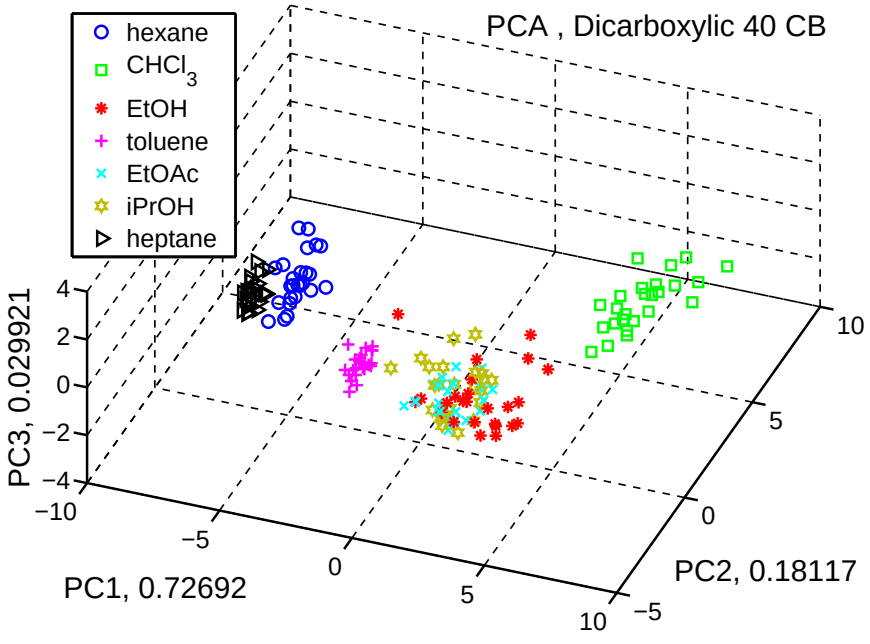

Figure 4.10: PCA plot of dicarboxylic acid 40 CB sensors. There are 25 exposures to each analyte. Numbers next to each principal component axis reflect the percentage of the total sensor response variance contained in that principal component

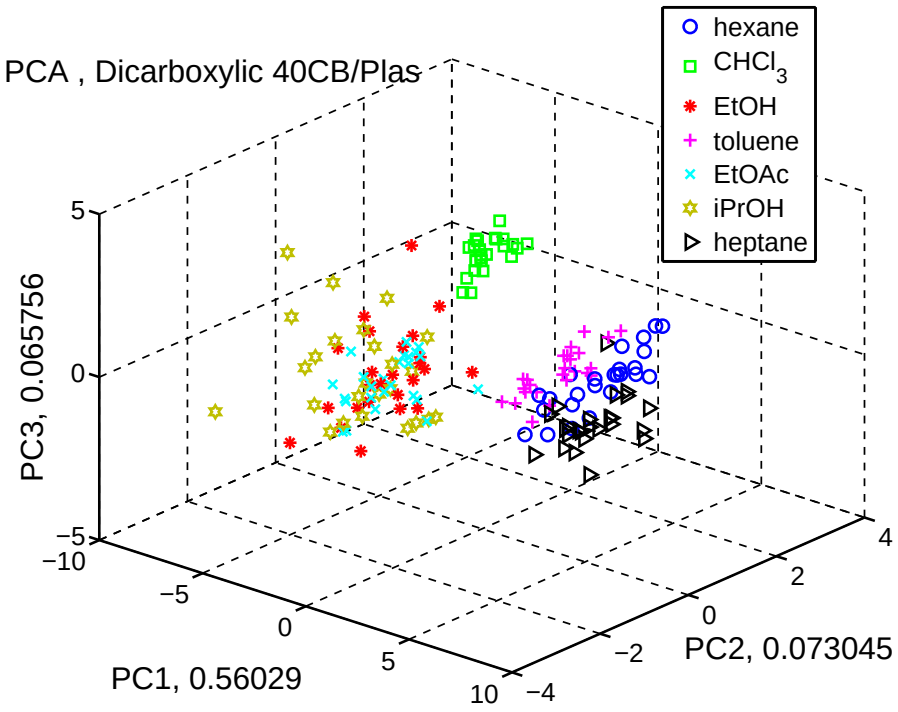

Figure 4.11: PCA plot of dicarboxylic acid 40/p sensors. There are 25 exposures to each analyte. Numbers next to each principal component axis reflect the percentage of the total sensor response variance contained in that principal component

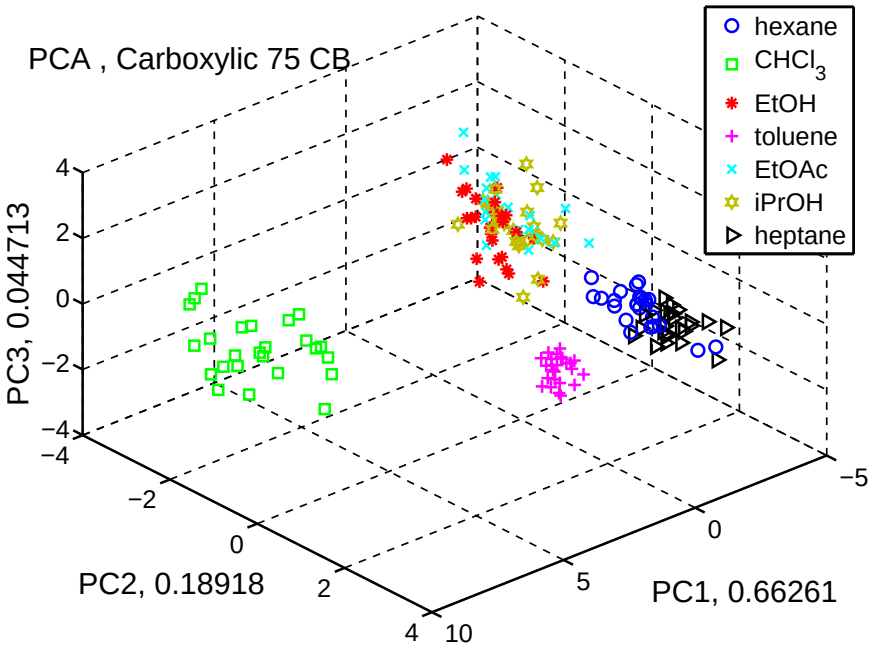

Figure 4.12: PCA plot of carboxylic acid 75 CB sensors. There are 25 exposures to each analyte. Numbers next to each principal component axis reflect the percentage of the total sensor response variance contained in that principal component

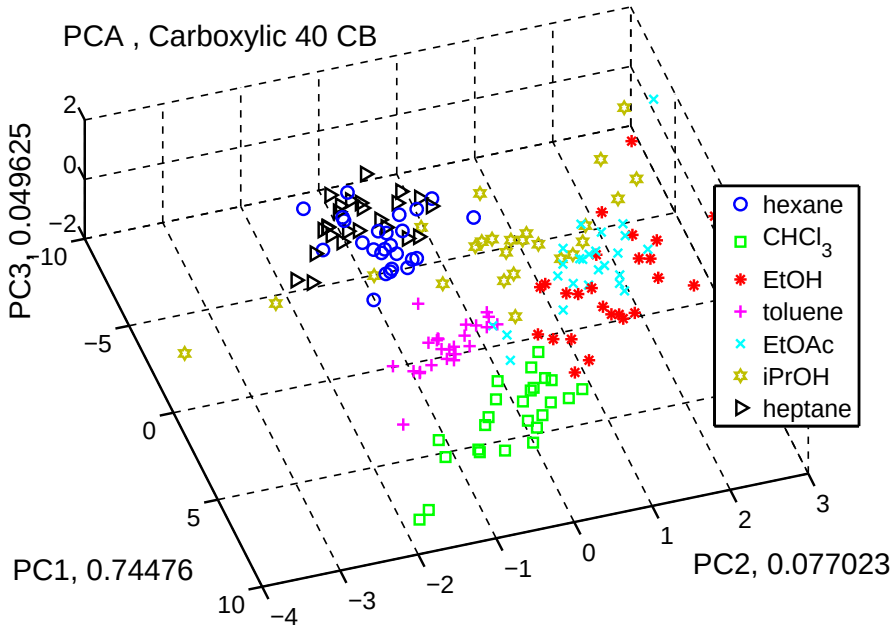

Figure 4.13: PCA plot of carboxylic acid 40 CB sensors. There are 25 exposures to each analyte. Numbers next to each principal component axis reflect the percentage of the total sensor response variance contained in that principal component

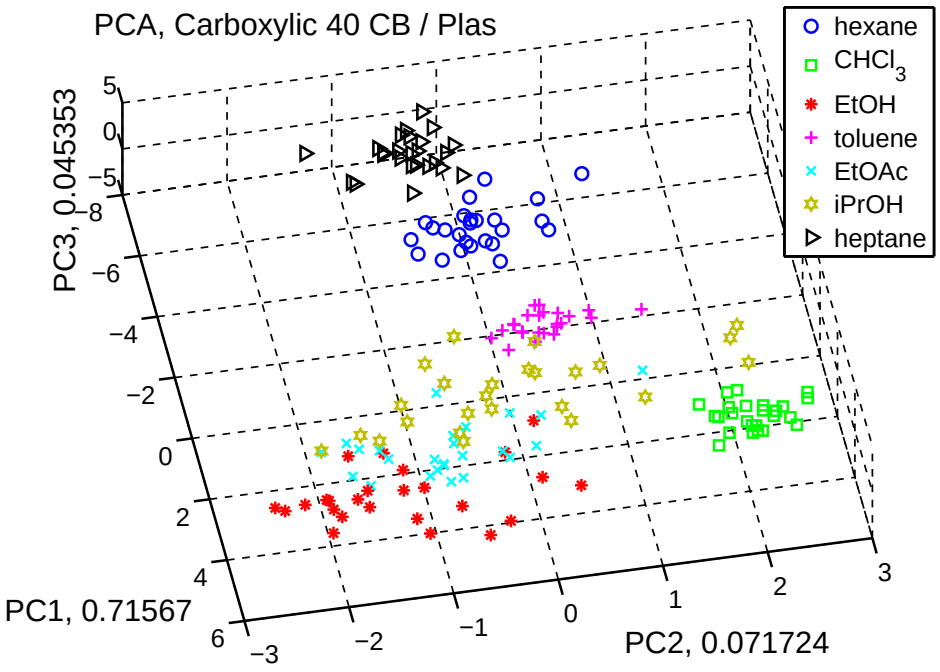

Figure 4.14: PCA plot of carboxylic acid 40/p sensors. There are 25 exposures to each analyte. Numbers next to each principal component axis reflect the percentage of the total sensor response variance contained in that principal component

CB%	Dicarb. acid	hexane	heptane	toluene	chloroform	EtOH	iPrOH	EtOAc
75	C2	0.52 ± 0.30	0.59 ± 0.28	1.59 ± 0.27	0.09 ± 0.22	1.69 ± 0.17	2.00 ± 0.19	2.86 ± 0.22
	C4	2.32 ± 0.03	3.11 ± 0.31	4.00 ± 0.27	2.02 ± 0.13	1.50 ± 0.21	1.85 ± 0.17	2.22 ± 0.24
	C6	2.36 ± 0.30	3.12 ± 0.26	4.27 ± 0.26	2.14 ± 0.14	1.67 ± 0.23	2.06 ± 0.18	2.46 ± 0.26
	C8	1.87 ± 0.24	2.28 ± 0.21	3.73 ± 0.23	2.66 ± 0.11	1.67 ± 0.19	1.91 ± 0.16	2.45 ± 0.16
	C10	1.71 ± 0.20	2.01 ± 0.18	3.36 ± 0.19	2.39 ± 0.10	1.36 ± 0.15	1.62 ± 0.12	1.97 ± 0.12
	C12	1.59 ± 0.23	1.91 ± 0.24	3.30 ± 0.28	2.34 ± 0.12	1.40 ± 0.18	1.65 ± 0.15	2.04 ± 0.18
	C14	1.49 ± 0.21	1.81 ± 0.23	3.20 ± 0.27	1.79 ± 0.13	1.36 ± 0.17	1.62 ± 0.14	1.96 ± 0.17
40	C2	1.80 ± 0.25	2.47 ± 0.20	3.67 ± 0.26	1.10 ± 0.25	1.13 ± 0.25	1.24 ± 0.10	1.65 ± 0.15
	C4	3.56 ± 0.20	4.74 ± 0.31	4.36 ± 0.20	1.42 ± 0.11	0.73 ± 0.16	0.80 ± 0.10	1.04 ± 0.14
	C6	2.12 ± 0.10	2.75 ± 0.11	3.86 ± 0.09	1.96 ± 0.08	1.12 ± 0.12	1.18 ± 0.08	1.49 ± 0.10
	C8	0.94 ± 0.07	1.09 ± 0.06	2.17 ± 0.07	1.55 ± 0.04	0.79 ± 0.07	0.79 ± 0.07	1.04 ± 0.08
	C10	1.22 ± 0.08	1.46 ± 0.08	2.84 ± 0.08	1.85 ± 0.06	0.91 ± 0.10	0.93 ± 0.07	1.22 ± 0.08
	C12	0.90 ± 0.05	1.02 ± 0.06	1.98 ± 0.06	1.69 ± 0.04	0.78 ± 0.08	0.79 ± 0.06	1.01 ± 0.06
	C14	0.64 ± 0.05	0.69 ± 0.06	1.43 ± 0.05	1.50 ± 0.09	0.71 ± 0.06	0.72 ± 0.06	0.90 ± 0.06
40/p	C2	2.42 ± 0.20	2.78 ± 0.22	3.48 ± 0.21	3.21 ± 0.19	1.11 ± 0.21	1.03 ± 0.15	1.49 ± 0.18
	C4	2.37 ± 0.27	2.93 ± 0.30	3.44 ± 0.29	2.28 ± 0.25	1.20 ± 0.27	1.24 ± 0.21	1.69 ± 0.23
	C6	1.78 ± 0.22	2.02 ± 0.25	2.69 ± 0.23	2.75 ± 0.22	0.99 ± 0.17	0.93 ± 0.15	1.30 ± 0.21
	C8	1.23 ± 0.16	1.28 ± 0.19	1.90 ± 0.17	2.25 ± 0.19	0.87 ± 0.17	0.69 ± 0.14	1.13 ± 0.16
	C10	1.01 ± 0.21	0.92 ± 0.27	1.72 ± 0.25	2.97 ± 0.27	0.98 ± 0.21	0.74 ± 0.20	1.21 ± 0.24
	C12	1.17 ± 0.23	1.19 ± 0.27	1.73 ± 0.23	2.58 ± 0.27	0.89 ± 0.21	0.71 ± 0.20	1.11 ± 0.26
	C14	0.99 ± 0.15	0.95 ± 0.16	1.53 ± 0.15	2.55 ± 0.22	0.81 ± 0.14	0.75 ± 0.14	1.05 ± 0.15

Table 4.3: $\Delta R_{\max}/R_{\mathrm{b}}$ values x 1,000 for all dicarboxylic acids measured in this study. Data are means obtained from 25 exposures to a given analyte. The reported error is one standard deviation.

CB%	Dicarb. acid	hexane	heptane	toluene	chloroform	EtOH	iPrOH	EtOAc
75	C2	17 ± 12	23 ± 17	35 ± 24	1 ± 13	48 ± 29	62 ± 54	68 ± 53
	C4	60 ± 28	83 ± 41	100 ± 63	48 ± 35	44 ± 28	52 ± 20	62 ± 37
	C6	59 ± 22	82 ± 35	148 ± 80	74 ± 47	58 ± 28	82 ± 59	72 ± 41
	C8	93 ± 38	92 ± 47	160 ± 49	257 ± 106	72 ± 29	131 ± 144	81 ± 22
	C10	83 ± 37	102 ± 44	122 ± 56	128 ± 62	57 ± 20	71 ± 29	68 ± 22
	C12	77 ± 34	98 ± 46	215 ± 282	220 ± 173	62 ± 31	105 ± 81	113 ± 219
	C14	58 ± 31	75 ± 38	169 ± 136	91 ± 53	58 ± 42	81 ± 57	62 ± 18
40	C2	63 ± 30	86 ± 49	112 ± 45	22 ± 17	35 ± 18	40 ± 15	59 ± 28
	C4	110 ± 65	132 ± 52	91 ± 47	50 ± 30	24 ± 18	34 ± 13	39 ± 19
	C6	140 ± 49	177 ± 93	212 ± 85	155 ± 90	50 ± 13	104 ± 91	85 ± 34
	C8	50 ± 32	47 ± 16	98 ± 25	74 ± 24	41 ± 14	49 ± 20	51 ± 24
	C10	89 ± 82	96 ± 37	133 ± 78	121 ± 51	59 ± 28	68 ± 42	67 ± 23
	C12	51 ± 19	62 ± 36	118 ± 94	84 ± 30	53 ± 30	41 ± 19	47 ± 15
	C14	36 ± 11	47 ± 18	77 ± 25	76 ± 35	54 ± 25	55 ± 26	58 ± 27
40/p	C2	118 ± 35	146 ± 88	161 ± 51	163 ± 64	54 ± 26	55 ± 20	76 ± 21
	C4	27 ± 9	36 ± 14	45 ± 40	28 ± 13	15 ± 8	18 ± 6	20 ± 10
	C6	21 ± 8	22 ± 7	26 ± 12	27 ± 10	15 ± 9	12 ± 8	16 ± 10
	C8	39 ± 17	39 ± 19	59 ± 24	78 ± 33	30 ± 14	25 ± 14	33 ± 15
	C10	18 ± 16	15 ± 8	25 ± 11	47 ± 37	15 ± 4	11 ± 5	17 ± 5
	C12	9 ± 4	9 ± 5	13 ± 4	23 ± 10	8 ± 3	5 ± 2	10 ± 6
	C14	28 ± 13	36 ± 15	52 ± 29	98 ± 65	34 ± 18	24 ± 13	31 ± 9

Table 4.4: SNR for all dicarboxylic acids measured in this study. Data are means obtained from 25 exposures to a given analyte. The reported error is one standard deviation.

CB%	Carb. acid	hexane	heptane	toluene	chloroform	EtOH	iPrOH	EtOAc
75	C10	3.42 ± 0.22	4.49 ± 0.23	5.25 ± 0.18	1.76 ± 0.24	1.67 ± 0.29	1.76 ± 0.20	2.29 ± 0.14
	C14	2.46 ± 0.16	3.06 ± 0.15	4.19 ± 0.11	2.65 ± 0.18	0.89 ± 0.22	0.95 ± 0.14	1.18 ± 0.11
	C16	2.36 ± 0.20	3.12 ± 0.22	3.98 ± 0.25	1.90 ± 0.22	1.06 ± 0.24	1.12 ± 0.18	1.35 ± 0.14
	C18	1.99 ± 0.22	2.66 ± 0.25	3.69 ± 0.21	1.36 ± 0.27	1.35 ± 0.28	1.44 ± 0.24	1.72 ± 0.18
	C24	1.88 ± 0.18	2.60 ± 0.25	3.43 ± 0.22	1.20 ± 0.25	0.90 ± 0.21	0.99 ± 0.17	1.16 ± 0.15
40	C10	4.07 ± 0.23	5.11 ± 0.19	5.46 ± 0.20	2.29 ± 0.23	1.19 ± 0.26	2.14 ± 0.16	2.55 ± 0.18
	C14	0.66 ± 0.12	0.68 ± 0.09	1.34 ± 0.08	0.96 ± 0.07	0.44 ± 0.11	0.37 ± 0.09	0.55 ± 0.08
	C16	0.52 ± 0.08	0.57 ± 0.06	1.17 ± 0.05	0.82 ± 0.06	0.39 ± 0.09	0.31 ± 0.07	0.47 ± 0.07
	C18	0.62 ± 0.07	0.66 ± 0.07	1.42 ± 0.05	0.91 ± 0.04	0.44 ± 0.07	0.38 ± 0.06	0.52 ± 0.06
	C24	0.89 ± 0.10	0.97 ± 0.09	2.01 ± 0.07	1.34 ± 0.08	0.56 ± 0.11	0.53 ± 0.09	0.69 ± 0.08
40/p	C10	3.50 ± 0.32	4.53 ± 0.30	4.81 ± 0.35	3.31 ± 0.30	1.07 ± 0.16	1.11 ± 0.21	1.40 ± 0.16
	C14	0.77 ± 0.12	0.79 ± 0.08	1.35 ± 0.11	1.37 ± 0.13	0.50 ± 0.07	0.40 ± 0.10	0.58 ± 0.08
	C16	0.77 ± 0.09	0.79 ± 0.07	1.43 ± 0.09	1.37 ± 0.09	0.46 ± 0.05	0.37 ± 0.07	0.53 ± 0.06
	C18	0.87 ± 0.09	0.90 ± 0.07	1.51 ± 0.10	1.63 ± 0.09	0.45 ± 0.08	0.38 ± 0.07	0.54 ± 0.08
	C24	0.85 ± 0.12	0.93 ± 0.12	1.41 ± 0.11	1.43 ± 0.13	0.42 ± 0.08	0.39 ± 0.11	0.51 ± 0.07

Table 4.5: $\Delta R_{\max}/R_{\mathrm{b}}$ values x 1,000 for all carboxylic acids measured in this study. Data are means obtained from 25 exposures to a given analyte. The reported error is one standard deviation.

CB%	Carb. acid	hexane	heptane	toluene	chloroform	EtOH	iPrOH	EtOAc
75	C10	275 ± 116	421 ± 337	645 ± 562	128 ± 56	93 ± 39	146 ± 77	109 ± 34
	C14	125 ± 44	187 ± 130	206 ± 83	165 ± 107	55 ± 28	66 ± 38	76 ± 31
	C16	36 ± 17	45 ± 20	62 ± 21	29 ± 11	21 ± 11	22 ± 9	26 ± 19
	C18	181 ± 149	144 ± 110	292 ± 318	65 ± 46	69 ± 29	89 ± 46	108 ± 115
	C24	62 ± 32	86 ± 56	104 ± 45	31 ± 22	33 ± 19	35 ± 22	40 ± 23
40	C10	137 ± 74	126 ± 41	157 ± 71	52 ± 24	52 ± 16	66 ± 30	70 ± 29
	C14	19 ± 8	18 ± 12	38 ± 12	26 ± 12	15 ± 10	11 ± 7	17 ± 8
	C16	21 ± 12	20 ± 6	44 ± 22	33 ± 21	17 ± 9	13 ± 6	16 ± 7
	C18	50 ± 17	51 ± 20	133 ± 69	81 ± 39	39 ± 24	34 ± 14	52 ± 29
	C24	28 ± 16	34 ± 16	62 ± 41	42 ± 17	19 ± 8	18 ± 9	21 ± 8
40/p	C10	508 ± 286	841 ± 629	651 ± 350	495 ± 374	116 ± 73	162 ± 78	135 ± 98
	C14	20 ± 9	21 ± 7	40 ± 15	35 ± 14	16 ± 7	13 ± 6	17 ± 7
	C16	37 ± 17	37 ± 14	70 ± 30	73 ± 33	24 ± 8	19 ± 8	19 ± 7
	C18	31 ± 13	36 ± 21	55 ± 32	51 ± 18	17 ± 5	20 ± 11	19 ± 7
	C24	56 ± 137	29 ± 15	42 ± 17	43 ± 21	15 ± 6	14 ± 6	19 ± 8

Table 4.6: SNR for all carboxylic acids measured in this study. Data are means obtained from 25 exposures to a given analyte. The reported error is one standard deviation.

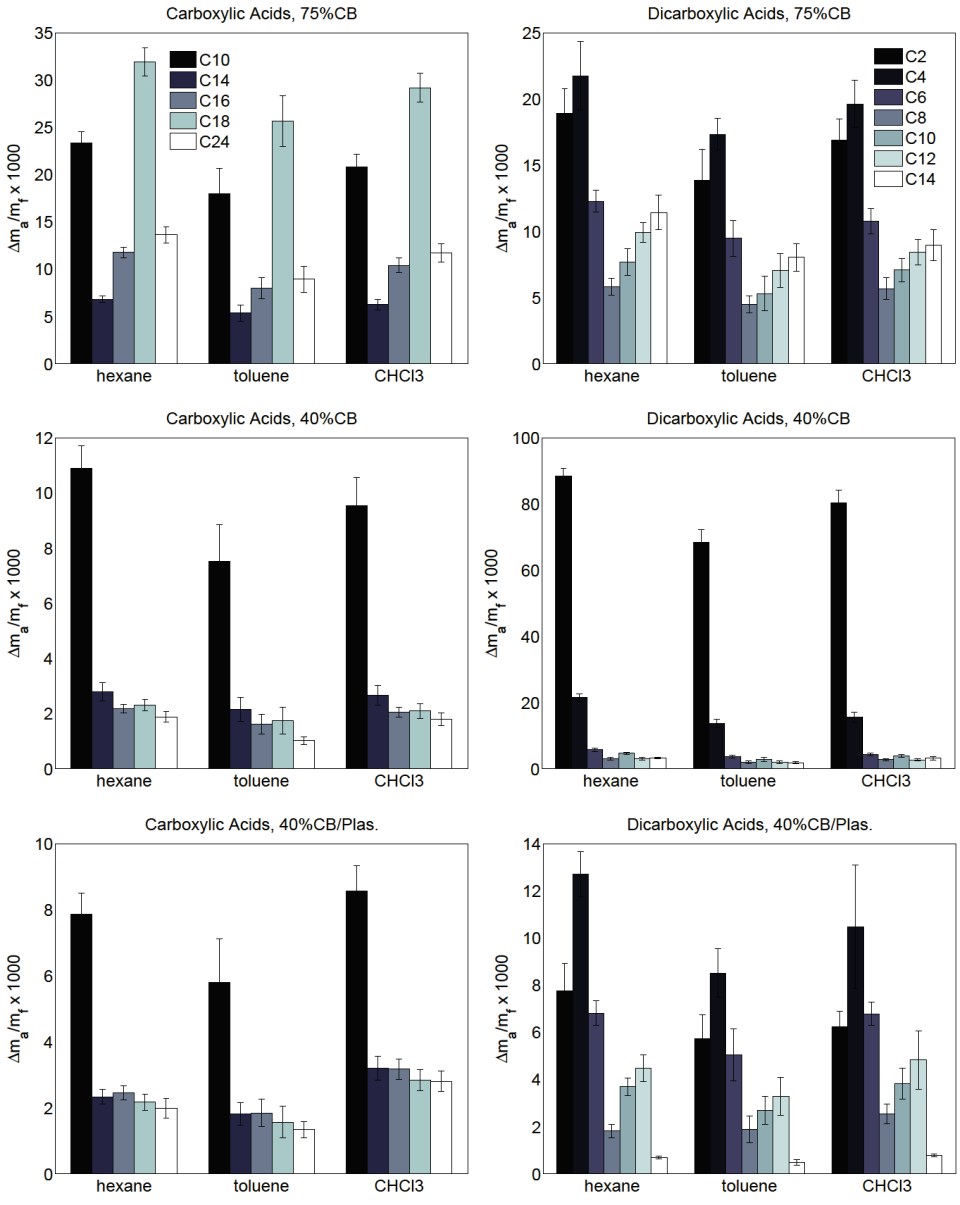

Figure 4.15: $\Delta m_{\mathrm{a}}/m_{\mathrm{f}}$ QCM values for all CB-containing films. Values are from the final run of each film, and are the average of 10 exposures to each analyte. Error is one standard deviation.

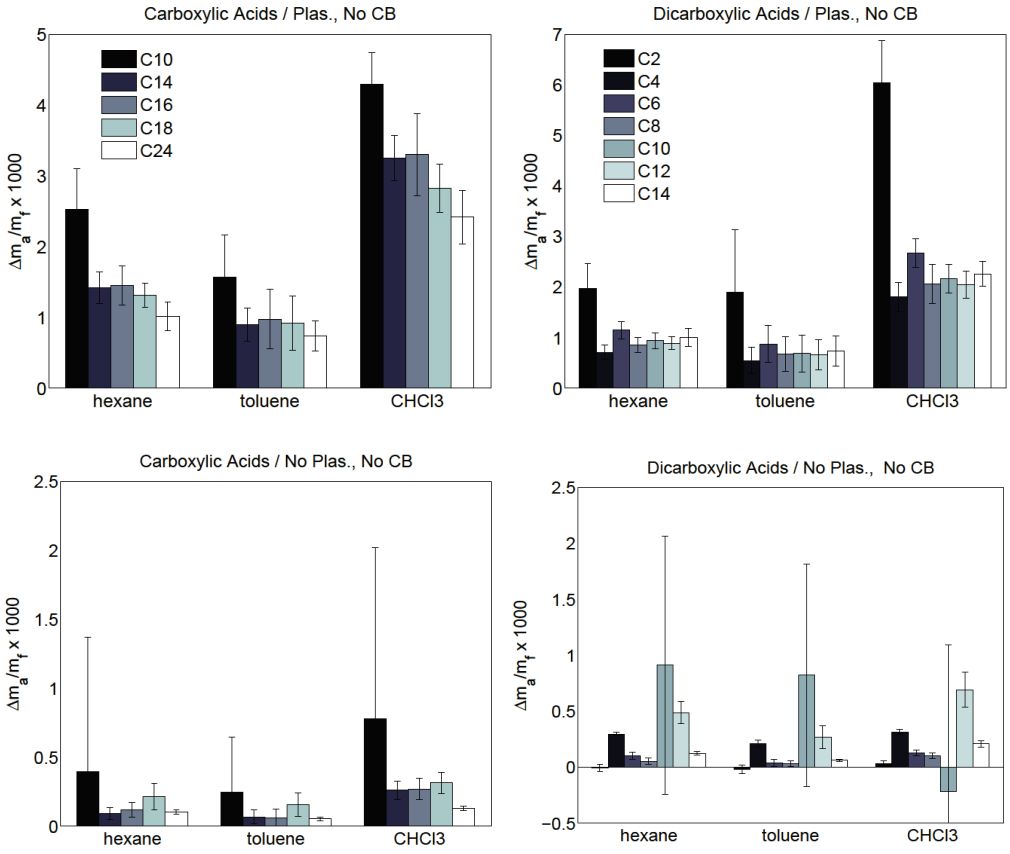

Figure 4.16: $\Delta m_{\mathrm{a}}/m_{\mathrm{f}}$ QCM values for all non-CB-containing films. Values are from the final run of each film, and are the average of 10 exposures to each analyte. Error is one standard deviation.

Acid Compound	No DOP Plasticizer			With Plasticizer		
	t (Å)	$\Delta h/h$ (%)	Δh (Å)	t (Å)	$\Delta h/h$ (%)	Δh (Å)
decanoic	-	-	-	-	-	-
myristic	361	2.4(0.7)	8.2(1.5)	388	5.5(0.3)	21.3(1.3)
	315	1.3(0.4)	4.0(1.2)	456	6.0(0.7)	27.5(3.4)
stearic	262	1.8(0.1)	5.3(1.1)	501	4.2(0.5)	21.0(2.8)
	252	2.0(0.4)	5.1(1.2)	295	8.1(0.3)	24.0(1.0)
palmitic	370	1.6(0.4)	6.0(1.6)	398	5.2(0.4)	19.8(1.5)
	311	1.4(0.1)	4.2(0.4)	474	7.4(0.3)	35.4(1.3)
tetracosanoic	275	2.4(0.4)	6.4(1.4)	440	8.1(0.3)	36.6(1.2)
	340	1.3(0.2)	4.3(0.6)	413	6.5(0.5)	30.3(2.0)
oxalic	204	1.7(0.3)	3.6(0.7)	208	16.9(1.9)	34.5(3.8)
	261	2.2(0.7)	5.7(2.0)	172	14.1(1.1)	23.7(1.5)
succinic	341	1.2(0.2)	3.9(0.6)	272	7.0(0.5)	18.9(1.4)
	204	4.2(0.2)	8.6(0.3)	383	9.2(0.3)	35.3(1.1)
adipic	330	1.7(0.2)	5.6(0.8)	456	5.6(0.2)	25.4(1.2)
	226	3.0(0.6)	7.5(0.3)	527	6.3(0.2)	33.1(1.3)
suberic	298	1.5(0.2)	4.4(0.6)	483	4.7(0.3)	22.7(1.5)
	337	1.6(0.1)	5.2(0.3)	504	6.1(0.4)	30.8(2.3)
sebacic	327	1.3(0.1)	4.1(0.4)	510	4.6(0.3)	23.3(1.8)
	387	1.3(0.2)	5.2(0.4)	553	4.0(0.3)	22.2(1.9)
dodecanedioic	334	1.4(0.2)	4.6(0.8)	426	6.1(0.6)	26.2(2.7)
	349	2.0(0.2)	6.9(0.6)	586	4.7(0.1)	27.6(0.9)
tetradecanedioic	332	0.7(0.1)	2.5(0.3)	465	5.7(0.3)	26.3(1.3)
	322	1.1(0.0)	3.6(0.1)	445	5.5(0.4)	25.5(2.1)
blank			5.1(0.4)			
			4.4(0.1)			
plasticizer				167	19.1(0.9)	31.7(1.6)
				162	23.4(0.6)	38.6(1.6)

Table 4.7: Averaged ellipsometry responses of carboxylic and dicarboxylic acid films. Reported error is one standard deviation. Decanoic acid films deposited by spin coating were not stable.

4.5 Discussion

Composite vapor sensors using small molecule substrates have several potential advantages over their polymer composite forebears. Unlike polymer composites, small molecule sensors almost uniformly function at very high carbon black loadings, both allowing decreased use of potentially expensive sensor materials and also hinting at an extremely high relative level of sensitivity. Greater disorder in small molecule films compared to polymer films and potentially higher functional group density have been theorized as causes for the high level of sensitivity. Additionally, use of small molecules allows access to a greater range of functional groups than can be achieved with polymers.

Here we see further confirmation of the sensitivity of the small molecule sensors. Sensor arrays composed of fixed terminal group, but varied chain length di- and monocarboxylic acids show good analyte discrimination. Moreover, accessibility of the small molecule functional groups is seen to aid discrimination, suggesting further use of multifunctional group small molecules to maximize overall discriminatory ability. However, we also see that volatility (both materially and behaviorally) of certain small molecules can lead to unpredictable results.

4.5.1 Small Molecule Responses — Size Variation

All small molecule sensors that produced reliable responses continued the trend of returning largest responses at the highest ratios of CB — i.e., using the smallest amount of responsive sensing material. This is directly counter to findings with polymer composite sensors in which addition of carbon black linearly decreases $\Delta R_{\max}/R_{\mathrm{b}}$ responses.[16] These

materials falling into this pattern provides further support to the theory (Chapter 2) that higher quantities of carbon black more effectively break up the small molecule crystalline structure, better allowing the composite material to swell.

However, very few effects were seen correlated to chain length differences. In the case of the carboxylic acids, the net effect of the increasing chain length from C14–C24 can be expected to be minimal, as there is still a singular carboxylic acid group, and a single alkyl tail, and the overall character of the molecules are similar (C10, however, exhibits distinct behavior, as discussed later). However, the increase in the length alkyl spacer in the dicarboxylic acids was expected to demonstrate a greater effect. Instead, the only clear trend is the increase in $\Delta R_{\text{max}}/R_{\text{b}}$ values of the C4–C8 dicarboxylic acids as compared to the longer chain molecules (oxalic acid, C2, also produced anomalous behavior, discussed later with decanoic acid). Above C8, the sensor responses were essentially flat.

Rather than increasing sensitivity to, e.g., the alkane analytes, an alternative idea is that the alkyl spacer instead provides a larger, flexible region where an analyte vapor can penetrate without displacing the molecule. In contrast, the shorter chain dicarboxylic acids can only accommodate the analyte vapors by physically separating, thus causing a greater physical shift in the CB particle network, and a concomitant increase in resistance. As all the carboxylic acids contain a large alkyl region, they would be less affected by this effect.

The shorter dicarboxylic acids also show somewhat increased mass uptake in QCM measurements (Figure 4.15) compared to the longer chain materials, but only in CB-containing films. While the reported $\Delta m_{\text{a}}/m_{\text{f}}$ values control for relative mass, the differing densities of the small molecules (Table 4.1) could cause volumetric sorption differences. How-

ever, the non-CB-containing QCM films (Figure 4.16), and ellipsometric measurement (Table 4.7), showed no trends correlated to chain length, suggesting that the response increases arises with the interplay between the acids and the carbon black, a set of interactions not yet well understood.

4.5.2 Functional Group Accessibility

While few intra-series differences were noted, clear differences were seen between the discriminating abilities of the carboxylic and dicarboxylic acid sensor arrays. The differences between the intermolecular hydrogen bonding abilities of the two series is clearly reflected in their relative melting points of the two sets of molecules (Table 4.1). As might be predicted from this difference, the dicarboxylic acids have a higher sensitivity to the oxygen-containing analytes than do the carboxylic acids, at all sensor formulations (Tables 4.3 and 4.5).

Despite this, however, only the carboxylic acid arrays demonstrated any ability to discriminate between the more polar analytes. Despite their overall increased density of carboxylic acid groups, PCA plots of all dicarboxylic acid array responses show no separation between EtOH/iPrOH/EtOAC (Figures 4.9 to 4.11). PCA plots of carboxylic accid arrays, however, display separation between these analytes, as well as showing increased separation between hexane and heptane (Figures 4.13 and 4.14). This is all the more remarkable given that there were only five chemically distinct sensors in the carboxylic acid arrays (although four copies of each sensor were present), and that four of those five sensors presented extremely similar sets of responses to each other (Figure 4.7, Table 4.5).

With both lowered overall responsiveness, and greater sensor similarity, carboxylic acids are still better able to discriminate between analytes than is a much more diverse set of dicarboxylic acids. One notable difference between the two sets of molecules is the greater accessibility of the alkyl group in the carboxylic acids. Analytes can interact with the carboxylic acid moiety, but also have free access to the alkyl tail. Compared to the dicarboxylic acids (or most polymeric materials) the analyte can interact with the sensor material in a more stereospecific fashion, allowing finer variations in response, as captured in PCA analysis.

Compared to a polymeric material, a linear small molecule offers greater access to at least two potentially distinct regions — the two ends. While the dicarboxylic acid responses suggest that the interior of a molecule may be blocked from exerting a significant influence, the potential to use a small molecule material with two (or more) distinct functional groups greatly increases the breadth of response available to a given size sensor array.

4.5.3 Unusual Responsiveness — Oxalic and Decanoic Acids

Responses of oxalic and decanoic acids highlight potential features and pitfalls of small molecules used in composite vapor sensors. Both materials — the smallest in each homologous series — displayed behaviors widely diverging from those of the rest of their series.

Decanoic acid reproducibly produced much higher $\Delta R_{\text{max}}/R_{\text{b}}$ values than did all other carboxylic acids, and also sorbed a greater quantity of analyte. However, this molecule is the shortest chain carboxylic acid that is solid at room temperature, and has a melting

point of 32 °C — only 10 °C above the normal laboratory operating conditions. The high responsiveness is thus partnered with a relatively large instability of the pure material, noted especially in the inability to cast ellipsometry films from this material.

Oxalic acid, while more stable in material properties than decanoic acid (with a melting point of 190 °C) proved, however, far more erratic in its responses. Response times and curve shapes of oxalic sensors differed widely from those of the other dicarboxylic acid sensors (Figure 4.3), even after their responses had stabilized over time (Figure 4.2). Oxalic acid, upon surface examination, would appear to have excellent potential to respond to polar analytes, but instead some combination of its own polarity, hydrogen bonding, hygroscopic nature, and other unusual properties leave it with untrustworthy responses.

The instability seen with these two molecules makes clear that the physical characteristics of potential small molecule sensor materials must be taken into consideration, beyond just the identity of their functional groups. The unusual response patterns evidenced by these two materials also shows, however, how very small apparent differences between two small molecules can yield highly varied sensor responses, further pointing out how small molecule composite sensors can aid in fine discrimination tasks in future sensor arrays.

4.6 Conclusions

Small molecule/CB composite vapor sensor arrays of two homologous series of small molecules (linear carboxylic and dicarboxylic acids) have been explored to better understand the effects of chain length and functional group presence in the performance of such sensors. Only minimal chain length effects were noted, although the smallest member of

each chain provided unexpected responses. Arrays comprised of carboxylic acids provided better analyte discrimination than did arrays of dicarboxylic acids, despite fewer distinct sensors in the carboxylic acid arrays. This greater availability of the alkyl group in the carboxylic acids as compared to the dicarboxylic acids could cause this effect. This points the way to new generations of highly sensitive small molecule sensors via selection of materials containing two or more accessible distinct functional groups.

4.7 Bibliography

[1] Young, R. C.; Buttner, W. J.; Linnell, B. R.; Ramesham, R. *Sens. Actuators, B* **2003**, *93*(1-3), 7–16.

[2] Ryan, M. A.; Shevade, A. V.; Zhou, H.; Homer, M. L. *MRS Bull.* **2004**, *29*(10), 714–719.

[3] Kateb, B.; Ryan, M. A.; Homer, M. L.; Lara, L. M.; Yin, Y. F.; Higa, K.; Chen, M. Y. *Neuroimage* **2009**, *47*, T5–T9.

[4] Dragonieri, S.; Schot, R.; Mertens, B. J. A.; Le Cessie, S.; Gauw, S. A.; Spanevello, A.; Resta, O.; Willard, N. P.; Vink, T. J.; Rabe, K. F.; Bel, E. H.; Sterk, P. J. *J. Allergy Clin. Immun.* **2007**, *120*(4), 856–862.

[5] Balasubramanian, S.; Panigrahi, S.; Kottapalli, B.; Wolf-Hall, C. E. *Lwt - Food Sci. Technol.* **2007**, *40*(10), 1815–1825.

[6] Ampuero, S.; Bosset, J. O. *Sens. Actuators, B* **2003**, *94*(1), 1–12.

[7] Toal, S. J.; Trogler, W. C. *J. Mater. Chem.* **2006**, *16*(28), 2871–2883.

[8] Senesac, L.; Thundat, T. G. *Mater. Today* **2008**, *11*(3), 28–36.

[9] Freund, M. S.; Lewis, N. S. *P. Natl. Acad. Sci. USA* **1995**, *92*(7), 2652–2656.

[10] Gardner, J. W.; Bartlett, P. N. *Synthetic Met.* **1993**, *57*(1), 3665–3670.

[11] Briglin, S. M.; Gao, T.; Lewis, N. S. *Langmuir* **2004**, *20*(2), 299–305.

[12] Kim, Y. J.; Yang, Y. S.; Ha, S. C.; Cho, S. M.; Kim, Y. S.; Kim, H. Y.; Yang, H.; Kim, Y. T. *Sens. Actuators, B* **2005**, *106*(1), 189–198.

[13] Wohltjen, H.; Snow, A. W. *Anal. Chem.* **1998**, *70*(14), 2856–2859.

[14] Philip, B.; Abraham, J. K.; Chandrasekhar, A.; Varadan, V. K. *Smart Mater. Struct.* **2003**, *12*(6), 935–939.

[15] Zhang, T.; Mubeen, S.; Myung, N. V.; Deshusses, M. A. *Nanotechnology* **2008**, *19*(33).

[16] Lonergan, M. C.; Severin, E. J.; Doleman, B. J.; Beaber, S. A.; Grubbs, R. H.; Lewis, N. S. *Chem. Mater.* **1996**, *8*(9), 2298–2312.

[17] Sisk, B. C.; Lewis, N. S. *Sens. Actuators, B* **2005**, *104*(2), 249–268.

[18] Gao, T.; Woodka, M. D.; Brunschwig, B. S.; Lewis, N. S. *Chem. Mater.* **2006**, *18*(22), 5193–5202.

[19] Severin, E. J.; Doleman, B. J.; Lewis, N. S. *Anal. Chem.* **2000**, *72*(4), 658–668.

[20] Burl, M. C.; Sisk, B. C.; Vaid, T. P.; Lewis, N. S. *Sens. Actuators, B* **2002**, *87*(1), 130–149.

[21] Briglin, S. M.; Lewis, N. S. *J. Phys. Chem. B* **2003**, *107*(40), 11031–11042.

[22] Bond, A. D. *Crystengcomm* **2006**, *8*(4), 333–337.

[23] Thalladi, V. R.; Nusse, M.; Boese, R. *J. Am. Chem. Soc.* **2000**, *122*(38), 9227–9236.

[24] Duda, R. O.; Hart, P. E.; Stork, D. G. *Pattern Classification;* Wiley: New York, 2nd ed., 2001.